Epileptic Spike Detection by Using a Linear-Phase Convolutional Neural Network

Kosuke Fukumori, *Student Member, IEEE,* Noboru Yoshida, Hidenori Sugano, Madoka Nakajima, and Toshihisa Tanaka, *Senior Member, IEEE*

***Abstract*—To cope with the lack of highly skilled professionals, machine leaning with proper signal techniques is a key to establishing automated diagnostic-aid technologies to conduct epileptic electroencephalogram (EEG) testing. In particular, frequency filtering with appropriate passbands is essential to enhance biomarkers—such as epileptic spike waves—that are noted in the EEG. This paper introduces a novel class of convolutional neural networks (CNNs) having a bank of linear-phase finite impulse response filters at the first layer. These may behave as bandpass filters that extract biomarkers without destroying waveforms because of linear-phase condition. The proposed CNNs were trained with a large amount of clinical EEG data, including 15,899 epileptic spike waveforms recorded from 50 patients. These have been labeled by specialists. Experimental results show that the trained data-driven filter bank with supervised learning is dyadic like discrete wavelet transform. Moreover, the area under the curve achieved above 0.9 in most cases.**

***Index Terms*—Epilepsy; Spike detection; Electroencephalogram (EEG); Linear-phase filter; Convolutional neural network (CNN).**

I. Introduction

EPILEPSY is a neurological disorder that is said to have 50 million patients worldwide. In particular, childhood epilepsy affects individual cognitive activity. Early appropriate diagnosis supports the patients to reduce future brain damage. In diagnosis, measurements taken using an electroencephalogram (EEG) along with a medical examination is essential to determine the type of seizure symptoms. Despite the fact that the examination requires clinical knowledge and experience, epilepsy specialists with these skills are chronically insufficient. This has motivated the development of an automated diagnostic aid to support epileptologists.

One of the important biomarkers in the diagnosis is an epileptic spike called a paroxysmal discharge, which is frequently recorded in a patient's interictal EEG. To support the detection of epileptic spikes, several automated detection manners are making great advances. To implement the automatic detection of epileptic spikes, supervised learning is one of the effective methods. To efficiently train the machine learning models, the signal of the EEG is generally decomposed into standard clinical bands of interest—such as δ, θ, α, β, and γ—before the learning [1]. While conducting such training,, it is necessary to appropriately select the frequency bands, which depend on a measurement method of the EEG and an individual patient. However, in various studies, a range of frequencies or frequency band of interest has been empirically selected. Douget et al. [2] used discrete wavelet transform (DWT) to obtain a set of sub-bands with a range of 4–32 Hz. Carey et al. [3] used an infinite impulse response Butterworth bandpass filter with a frequency band of 1–30 Hz.

With the advent of deep neural networks, models can learn from observation data, including the feature extraction method. In particular, convolutional neural networks extract features by applying filters to input data [4], [5]. However, each filter in the layer is fitted with a high degree of freedom in spite of the fact that the filters in the previous studies are designed with linear-phase constraints to preserve the waveform shape, which is also an essential requirement in the diagnosis by clinical experts, as filtering cannot destroy the shape of the signal to find epileptic biomarkers.

In this paper, we hypothesize that the frequency subbands can be estimated by the data from an epileptic EEG labeled by clinical specialists. To this end, we propose to use supervised learning to find filter coefficients regarded as a one-dimensional (1D) convolutional layer under a linear-phase constraint. This layer can be connected to general neural networks such as convolutional neural networks (CNNs) and artificial neural networks (ANNs) as a classifier. The proposed model is trained with a medical dataset containing spike waveforms of the EEG and the corresponding labels—either an epileptic spike or a non-epileptic discharge.

II. Related Work

A. Feature Extraction

Recently, many works that study epileptic EEGs have applied signal decomposition methods using DWT in a preprocessing stage [2], [6]–[12]. However, the parameter selection frequency range of bandpass filters is empirically given.

Cheong et al. [13] used DWT to decompose the signal into the frequency subbands from the delta band to the gamma band (0–63 Hz). Gutierrez et al. [6] applied a bandpass filter in the range of 0.5–70 Hz. Then, they obtained wavelet coefficients from the filterd signal to classify epileptic spikes. Similarly, the range of 0.5–70 Hz were extracted with a Butterworth filter to obtain wavelet coefficients [12].

Meanwhile, other studies utilized narrow bandpass filter ranges for preprocessing. Polat et al. [14] applied a bandpass

This work was supported by JST CREST Grant Number JPMJCR1784. The authors would like to thank Ms. Yuiko Kumagai for fruitful discussion on statistical analysis.

K. Fukumori and T. Tanaka are with the Tokyo University of Agriculture and Technology, Tokyo, Japan. T. Tanaka is also with RIKEN Center for Brain Science, Saitama, Japan and RIKEN Center for Advanced Intelligence Project, Tokyo, Japan.

N. Yoshida is with Juntendo University Nerima Hospital, Tokyo, Japan.

H. Sugano and M. Nakajima are with Juntendo University School of Medicine, Tokyo, Japan.

filter range of 0.53–40 Hz, and then used the discrete Fourier transform to extract features for the decision tree classifier. Khan et al. [9] used the range of 0–32 Hz decomposed by DWT since most of the epileptic information lies in 0.5–30 Hz. Similarly, Douget et al. [2] and Indiradevi et al. [15] adopted DWT with Daubechies 4 (DB4) to extract the frequency band of 4–32 Hz. Moreover, Fergus et al. [16] used the range of only 0–25 Hz, although they did not use DWT but a Butterworth filter. Thereafter, they employed the holdout technique and k-fold cross validation, passing into many different classifier models for distinguishing the seizure and non-seizure EEG records.

In these studies on the classification or detection of epilepsy, DWT decomposition and other filter methods were effective. However, the selection of filter range were set empirically in different studies. This motivated us to identify filter parameters from data.

B. Convolutional Neural Networks

One of the neural networks (NNs) that demonstrates excellent performance—especially in the field of image or video recognition [17], [18]—is a CNN. A CNN is an extended NN that has an input layer, multiple hidden layers, and an output layer. In general, the hidden layers consist of convolutional layers, and a fully connected layer is used as the output layer. The convolution layer applies a convolution to the input and forwards the result to the next layer. Let $X = \{x_0, x_1, \ldots, x_{N-1}\}$, $Y = \{y_0, y_1, \ldots, y_{M-1}\}$, and $H = \{h_0, h_1, \ldots, h_{L-1}\}$ be a 1D input signal, a 1D output signal, and a convolutional kernel, where N, M, and L are the length of X, Y, and H, respectively. For the sake of simplicity, L is assumed to be even. Focusing on one layer, the input X is convolved with the kernel H and the output Y is generated as follows:

$$y_m = \sum_{l=0}^{L-1} h_l x_{m-\frac{L}{2}+l}. \quad (1)$$

. The flattened layer smoothes multiple convolved signals into a single dimension. Then, the fully connected layer multiplies all input neurons by weight coefficients and connects them to the output.

Recently, some studies have applied a CNN to EEG signals [4], [5], [19], [20]. Ullah et al. [4] used 1D convolution to extract features by filtering time series EEG signals. Zhou et al. [20] directly input both of the multichannel time-series EEG signals and their frequency domain signals into a CNN. These studies, using CNN to detect epileptic seizures or epileptic spikes are gaining interest.

C. Dataset of Other Works

This section summarizes datasets of recent studies on epileptic spike detection. The most common task is the classification of epileptic spike waveforms and non-epileptic waveforms. Table I summarizes the datasets from similar studies. It should be emphasized that the dataset constructed in the current study achieved a much larger dataset (15,899 epileptic spike waveforms from 50 patients) than the conventional studies, where the largest one in terms of spike waveforms consists of 7,500 samples [19] and the one in terms of patients likewise consists of 50 patients [21].

TABLE I
SUMMARY OF THE DATASETS IN OTHER STUDIES ON EPILEPTIC SPIKE DETECTION

Reference and publication year	#Epileptic spikes	#Patients
Wilson et al. [21], 1999	2,400	50
Indiradevi et al. [15], 2008	684	22
Liu et al. [22], 2013	142	12
Johansen et al. [19], 2016	7,500	5
Douget et al. [2], 2017	2,157	17
Xuyen et al. [11], 2018	1,491	19
Thanh et al. [12], 2020	1,442	17
This paper	15,899	50

III. Method

A. Dataset

Table II datails the dataset. EEG recordings were collected from 50 patients (23 males 27 females) with benign epilepsy with centro-temporal spikes (BECTS) [23] at the Department of Pediatrics, Juntendo University Nerima Hospital. The age at the time of the examination was 3–12 years. The data were recorded with the international 10–20 methods using the Nihon Koden EEG-1200 system. The sampling frequency was 500 Hz. This dataset was recorded and analyzed under approval from the Juntendo University Hospital Ethics Committee and the Tokyo University of Agriculture and Technology Ethics Committee.

First, two neurosurgeons, one pediatrician, and two clinical technologists selected a focal channel associated with the origin of the epileptic spike. Typically, one EEG dataset may contain multiple epileptic focal channels, and annotators selected the most intense channel as the focal channel. Peaks (minima and maxima) of the EEG at the channel were detected by PeakUtils [24]. Second, the annotators labeled each peak as either an epileptic spike (spike or spike-and-wave) or non-epileptic discharge. At every detected peak, a 1-s segment was extracted, including 300 ms before and 700 ms after the peak. Fig. 1 illustrates an example of typical waveforms. Z-score normalization was applied with mean value and standard deviation for each segment. It should be noted that each segment represents one candidate spike.

B. Preprocessing and Subband Decomopsition

We considered two models as shown in Fig. 2. The first model uses a predefined bank of filters. It is based on the method adopted in several previous studies. The second model involves a special convolution layer called the LPCL when the parameters are searched based on the dataset.

1) Fixed approach: The first approach is to employ a hand-engineered preprocessing for each segment. DWT is applied to extract the subbands from the EEG. In this paper, the Daubechies wavelet of order 4 (DB4), which has been reported to be appropriate for analyzing EEG signals [2], [25], [26], is

TABLE II
DATASET INFORMATION OF 50 EPILEPTIC EEG DIAGNOSED WITH BECTS. THIS DATASET WAS LABELED BY TWO NEUROSURGEONS, TWO CLINICAL TECHNOLOGISTS, AND ONE PEDIATRICIAN. THE TOTAL NUMBER OF LABELED SAMPLES IS 31,437.

Patient ID	Age of years	Sex	Annotator	#Epileptic spikes	#Non-epileptic discharges	#Total
1	8	Male	Neurosurgeon 1	1,009	763	1,772
2	9	Female	Pediatrician	172	108	280
3	9	Female	Pediatrician	456	225	681
4	9	Male	Neurosurgeon 1	85	416	501
5	7	Female	Neurosurgeon 1	345	199	544
6	10	Male	Neurosurgeon 1	295	209	504
7	10	Male	Neurosurgeon 1	84	333	417
8	5	Male	Pediatrician	211	255	466
9	6	Male	Pediatrician	351	151	502
10	8	Female	Clinical technologist 1	655	189	844
11	11	Male	Pediatrician	318	85	403
12	6	Male	Neurosurgeon 1	232	289	521
13	9	Female	Neurosurgeon 1	129	245	374
14	7	Male	Neurosurgeon 1	105	207	312
15	9	Female	Clinical technologist 1	331	214	545
16	7	Female	Neurosurgeon 1	253	390	643
17	6	Female	Clinical technologist 1	166	297	463
18	7	Male	Clinical technologist 2	232	298	530
19	9	Female	Neurosurgeon 1	368	358	726
20	7	Male	Neurosurgeon 1	350	190	540
21	6	Female	Clinical technologist 1	440	244	684
22	6	Female	Pediatrician	939	692	1,631
23	8	Male	Neurosurgeon 1	495	239	734
24	10	Female	Neurosurgeon 1	341	303	644
25	6	Female	Neurosurgeon 2	412	94	506
26	8	Male	Neurosurgeon 1	294	292	586
27	11	Female	Neurosurgeon 1	295	335	630
28	6	Female	Neurosurgeon 1	159	355	514
29	9	Male	Neurosurgeon 1	408	389	797
30	11	Female	Neurosurgeon 1	175	340	515
31	7	Male	Neurosurgeon 1	142	283	425
32	7	Female	Clinical technologist 1	560	314	874
33	10	Female	Pediatrician	99	55	154
34	7	Female	Neurosurgeon 1	416	293	709
35	9	Male	Neurosurgeon 1	231	330	561
36	11	Female	Neurosurgeon 1	446	385	831
37	9	Male	Clinical technologist 1	282	112	394
38	6	Female	Pediatrician	315	301	616
39	10	Male	Clinical technologist 1	321	351	672
40	10	Male	Neurosurgeon 1	385	189	574
41	7	Female	Clinical technologist 1	72	369	441
42	12	Female	Neurosurgeon 1	355	342	697
43	7	Female	Pediatrician	261	321	582
44	10	Male	Pediatrician	287	509	796
45	3	Male	Pediatrician	271	511	782
46	5	Male	Pediatrician	240	580	820
47	6	Male	Pediatrician	263	629	892
48	7	Female	Pediatrician	424	178	602
49	10	Female	Pediatrician	188	321	509
50	10	Female	Pediatrician	236	461	697
Total		23 males 27 females	24 by neurosurgeon 1 1 by neurosurgeon 2 8 by clinical technologist 1 1 by clinical technologist 2 16 by pediatrician	15,899	15,538	31,437

adopted as the mother wavelet. The input EEG is decomposed into six coefficient levels—D6, D5, D4, D3, D2, and D1—and one approximation level A6. Then, four subbands corresponding to D6, D5, D4, or D3 were generated. Each subband represents the θ band (4–8 Hz), the α band (8–16 Hz), the β band (16–32 Hz), the γ band (32–64 Hz), respectively [13]. The approximation level A6 and the coefficient levels D2 and D1 were eliminated because the low frequency band may include breathing and eye movements, and the high frequency band can be considered as noise.

2) Novel data-driven approach using linear-phase convolutional layer: Convolutional layer described in Section II-B can behave as a finite impulse response (FIR) filter. However, each weight in a convolutional layer is fitted with a high degree of freedom in spite of the fact that FIR filters are designed with linear-phase constraint in order to preserve the waveform shape. In this paper, we propose a convolutional layer with linear-phase constraints, called the *linear-phase convolutional*

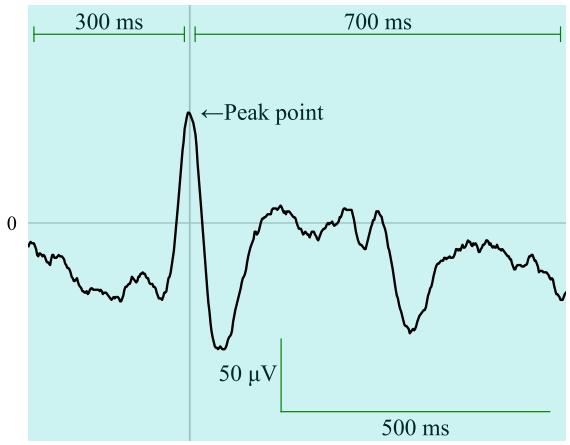

(a) An epileptic spike

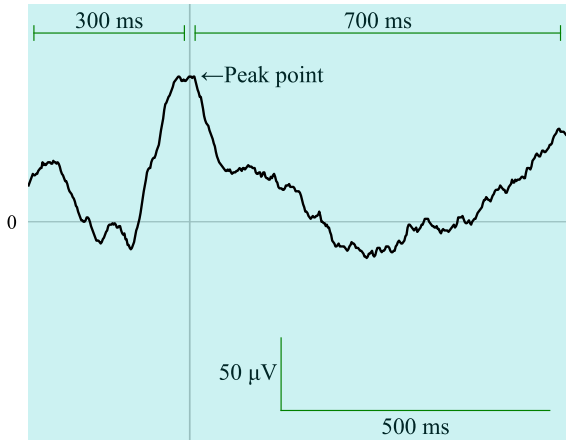

(b) A non-epileptic discharge

Fig. 1. Typical waveforms of detected peaks. Each waveform is clipped into 1-s segment.

layer (LPCL), and its implementation.

FIR filter is realized by convolution of the discrete signal $X = \{x_0, x_1, \ldots, x_{N-1}\}$ and the kernel $H = \{h_0, h_1, \ldots, h_{L-1}\}$, and the output discrete signal $Y = \{y_0, y_1, \ldots, y_{M-1}\}$ is calculated based on the current and past $L-1$ inputs as follows:

$$y_m = \sum_{l=0}^{L-1} h_l x_{m-l}. \tag{2}$$

Generally, the kernel described above causes phase distortion, which can be avoided by a linear-phase constraint. The even-symmetry or odd-symmetry of the kernel yields the linear-phase FIR filter, that is:

$$h_l = h_{L-1-l}, \tag{3}$$

or

$$h_l = -h_{L-1-l}. \tag{4}$$

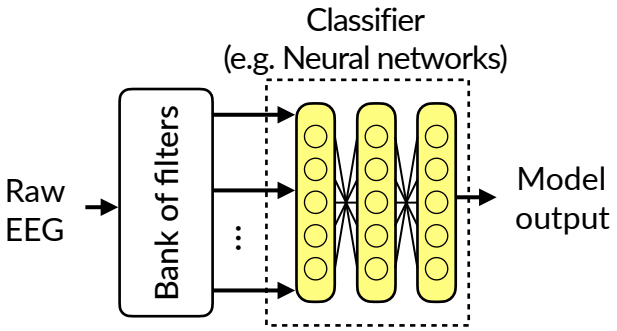

(a) The traditional fixed approach

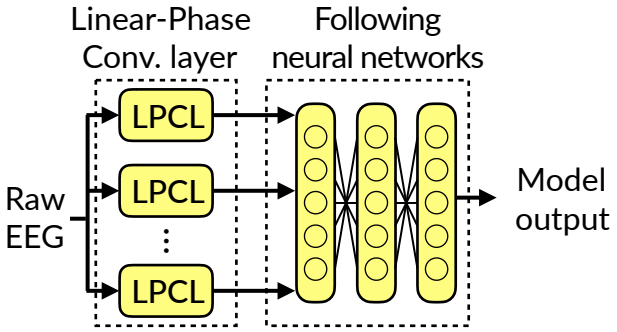

(b) The data-driven approach using the linear-phase convolutional layers

Fig. 2. The diagrams of the two prediction models. The colored blocks contain parameters to be trained.

From (2) and (3), an even-symmetric convolution $Y^e = \{y_0^e, y_1^e, \ldots, y_M^e\}$ is described as:

$$y_m^e = \sum_{l=0}^{L/2-1} h_l \left(x_{m+l} + x_{m+(L-1)-l}\right). \tag{5}$$

This convolution can be implemented by a butterfly structure, as shown in Fig. 3(a). As shown in this figure, even-symmetric convolution can be regarded as the product of the vector expressed by addition of the two components in X and the kernel H. This is the same operation as a weighted full connection (namely, a fully connected layer). Therefore, it can be implemented by repurposing a conventional neural network framework with the pre-addition of X. Similarly, an odd-symmetric convolution $Y^o = \{y_0^o, y_1^o, \ldots, y_M^o\}$ is described as:

$$y_m^o = \sum_{l=0}^{L/2-1} h_l \left(x_{m+l} - x_{m+(L-1)-l}\right). \tag{6}$$

Fig. 3(b) shows the butterfly structure for (6). As this figure shows, it can be implemented by repurposing a conventional neural network framework with the pre-subtraction of X. These LPCLs can replace the fixed (pre-designed) subband filters, as illustrated in Fig. 2. The underlying idea behind of using the LPCL is to hypothesize thet frequency bands of interest can be derived from the epileptic EEG dataset.

C. Classifier Models

Random forest (RF), artificial neural network (ANN), and CNN are adopted as the classifiers. Although, an ANN and a CNN can be combined with either a traditional preprocessing

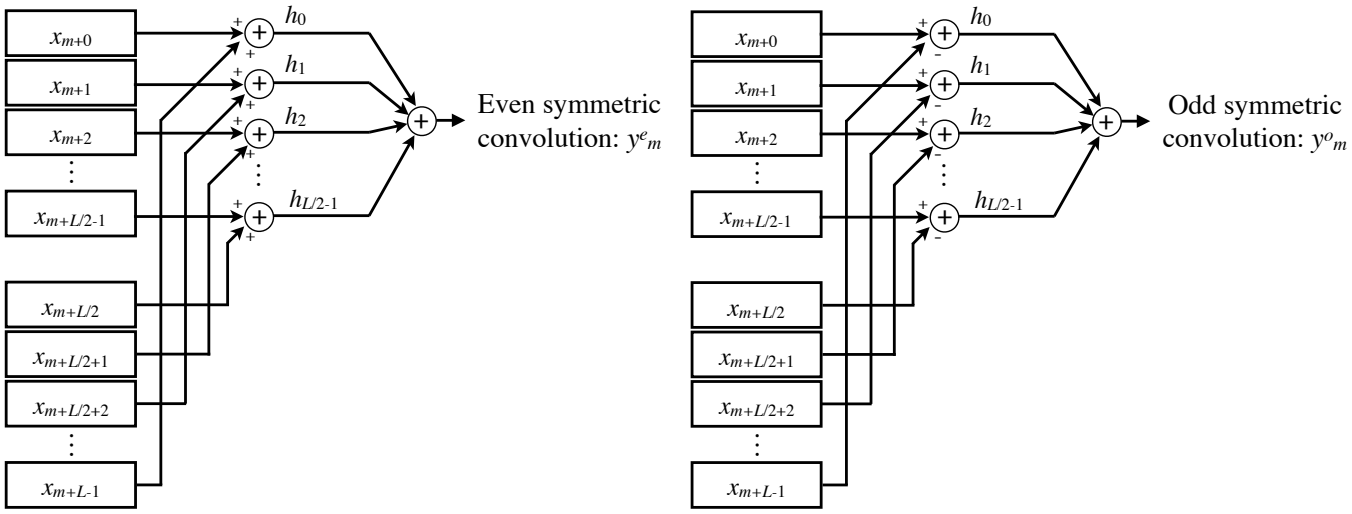

(a) Even symmetric convolution

(b) Odd symmetric convolution

Fig. 3. Butterfly structures of the linear-phase convolution.

TABLE III
PARAMETER FOR RANDOM FOREST TO BE TUNED BY GRID SEARCH

Parameter	Candidates
Number of trees N_{tree}	5, 10, 20, 30, 50, 100, 300
Maximum depth $D_{\max}$	2, 4, 6, 8, 10

or the proposed method, RF can be combined only with the traditional preprocessing.

The parameters for RF is tuned by a grid search for parameters listed in Table III. For adjusting the grid search, the F1-score is used as the ranking score and the five-fold cross validation with two subsets is used. The model architectures of ANN and CNN are depicted in Fig. 4. For the generation of initial weights of these models, the He initializer [27] is used for the layers that employ the rectified linear unit (ReLU) as the activation function, and the Xavier initializer [28] is used for the other layers.

D. Application of Linear-Phase Convolutional Layer

The total number of LPCLs shown in Fig. 2(b) is 10, and each filter setting is as shown in Table IV. The reason that there are LPCLs with different filter lengths is to let the model determine the appropriate filter length. The learning step is roughly divided into the following two parts:

1) Update only the coefficients of the LPCLs.
2) Update all coefficients of the main layers of the "Following neural networks" in Fig. 2(b).

The first step assists the learning of the filter coefficients in the added convolutional layer to extract the effective frequency bands from the raw signal in a stable manner, without the influence of the learning of the following network. Then, in the next step, the main layers are tuned to extract the hidden features in the signal.

IV. EXPERIMENTAL RESULT

To validate the effectiveness of the proposed method, an experiment is performed using the dataset described in Section III-A. Recall that the classification is binary: an epileptic spike or a non-epileptic discharge. For comparison, two approaches are used: the fixed approach (combined with RF, ANN and CNN) and the proposed data-driven approach (combined with ANN and CNN). In the fixed approach, a raw EEG is decomposed into four frequency bands using DWT.

TABLE IV
SETTINGS OF THE LPCLS

LPCL No.	Filter length	Constraint type
1	2	Even-symmetric
2	4	
3	8	
4	16	
5	32	
6	2	Odd-symmetric
7	4	
8	8	
9	16	
10	32	

In the experiment, inter-subject validation in all combinations are performed, where 49 patients are used as training data and the remaining patient is used as test data. For the evaluation of the models, the area under the curve (AUC) is employed. AUC is the area of the curve drawn by the false positive rate (FPR) and the true positive rate (TPR) when the discrimination threshold is changed, and is calculated in the following manner:

$$\mathrm{FPR} = \frac{\mathrm{FP}}{\mathrm{FP}+\mathrm{TN}},$$
$$\mathrm{TPR} = \frac{\mathrm{TP}}{\mathrm{TP}+\mathrm{FN}},$$

where TP, FP, FN, and TN are the numbers of true positive, false positive, false negative, and true negative, respectively. In particular, ANN and CNN evaluations use the mean AUC (by taking 30 independent realizations) because the initial weight or initial kernel value affect the learning. In addition, since the convolution filter can be regarded as a FIR filter,

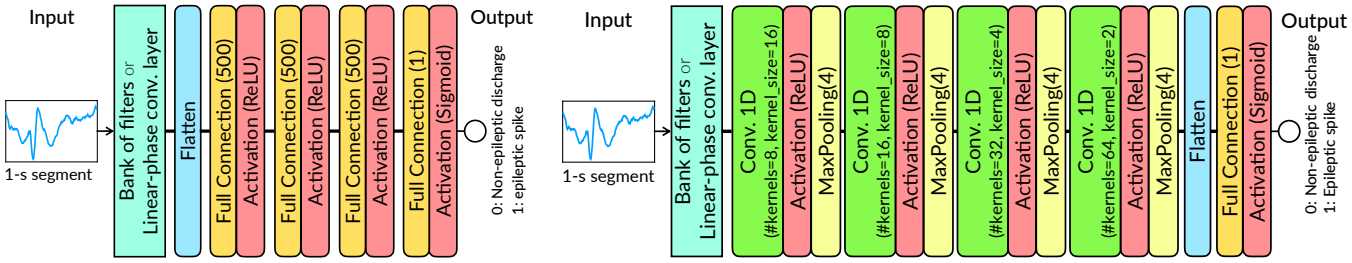

(a) Classification model based on ANN (b) Classification model based on CNN

Fig. 4. The model architectures. The input is decomposed by DWT or the linear-phase convolutional layer.

the frequency response of each filter of the 10 linear-phase convolutional layers is analyzed after training. Similar to the AUC evaluation, the frequency response are averaged by 30 independent runs.

Table V represents the AUC by each model and preprocessing. A statistical tests including Friedman's one-way analysis of variance (ANOVA) [29] showed that the effect of the models on the AUC was significant, $F_{(1,3)} = 104$, $p = 1.51 \times 10^{-22}$. Since the main effect of the models has been observed, Bonferroni *post-hoc* test [29] werwase performed to better understand the changes on cross-correlation across the different models. Fig. 5 visualizes the AUC results and its analysis of variance. As shown in Fig. 5, the AUC resuluts by LPCL + CNN were significantly different than the AUC resuluts by DWT + ANN ($p = 2.87 \times 10^{-6}$) and LPCL + ANN ($p = 3.23 \times 10^{-11}$). Moreover, the AUC resuluts by DWT + CNN were significantly different than the AUC results by DWT + ANN ($p = 1.08 \times 10^{-11}$) and LPCL + ANN ($p = 3.12 \times 10^{-18}$). Therefore, there is no significant effect of the change to LPCL since the CNN-based models show high AUC resuluts independent of the preprocessing.

Fig. 6 and Fig. 7 show examples of the frequency responses at the proposed layers. From Table V, it is clear that the AUC evaluation of the proposed method is comparable that achieved with traditional methods [2]. In addition, it is clear that the proposed method filter emphasizes the low frequency band (around 15 Hz) from Figs. 6 and 7. Thus, while the conventional method manually focuses on the low frequency band, it can be said that the proposed method automatically extracts this frequency. Moreover, from Figs. 6(b) and 7(b), it can be seen that filters with odd-symmetric constraints pass different frequency bands according to the filter length. Fig. 8 provides an example of prediction by CNN combined with the LPCL. From this figure, it is considered that a relatively sharp waveform is classified as an epileptic spike.

V. Discussion and Conclusion

The experimental results show that the filters with an odd symmetry constraint have a different passband respectively as shown in Figs. 6 and 7. This behavior is similar to the discrete wavelet transform. For example, the peak frequencies of the five spectra shown in Fig. 6(b) (the spectra by LPCL No. 6 to 10) are 14.6, 22.5, 47.4, 92.3, and 249 Hz, respectively. It can be seen that the frequencies at the peaks in spectrum of middle range were about half of that in high range. LPCL No. 6–8 can be considered to correspond to the standard clinical frequency bands of α, β, and γ, respectively. These results, which show that the filters learned from the raw EEG and the expert annotations are decomposed into their respective frequency bands, may support the validity of the other studies using DWT to decompose the EEG into clinical frequency bands [2], [25], [26]. Also, this finding may suggest that the filter emulates physician's analyze logic.

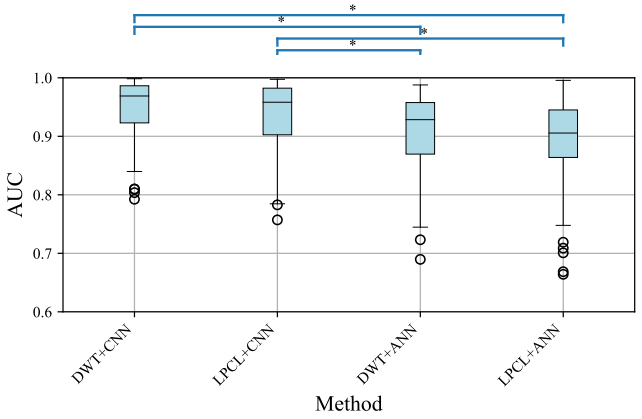

Fig. 5. Visualized AUC results shown in Table. V. Statistical significance is indicated by asterisk (*: $p < 0.01$).

Next, we investigated the characteristics of the 1-s segments in order to consider the effectiveness of the frequency band extracted by the LPCLs. To obtain the differences of spectra between the non-epileptic discharge segments and the epileptic spike segments, statistical analyses were performed on the amplitude distributions at each frequency by using Welch's t-test [30]. Next, the effect sizes were calculated using Cohen's d [31]. Fig. 9 shows the mean spectrum of all 15,538 non-epileptic discharges, the mean spectrum of all 15,899 epileptic spikes, the areas where $p < 0.01$ in the t-test, and the effect sizes. From Fig. 9, it can be seem that there is a significant difference across almost all frequencies. In addition, in the range of 5–15 Hz, there is a large difference ($d \approx 0.8$) between the two classes. As these results, it can be said that the LPCL, which has a maximum frequency response around 14 Hz, effectively extracted the low frequency band where there is a statistical difference, as shown in Fig. 6(b). Therefore, this result supports the effectiveness of low-pass filters in spike detection of epileptic EEG.

TABLE V
AUC EVALUATION RESULTS. FOR ANN OR CNN MODELS, THE AVERAGE OF 30 INDEPENDENT RUNS IS CALCULATED (MEAN AUC ± STD.

Patient ID		Classifier				
		Random forest	ANN	CNN	ANN	CNN
		Preprocessor				
Train data	Test data	DWT (Extraxt predefined frequency band: 4–64 Hz)			LPCL (Learn frequency band from the train data)	
All IDs except test data in the right column	1	0.998	0.970 ± 1.14E-02	0.995 ± 2.37E-03	0.996 ± 9.59E-04	0.997 ± 8.10E-04
	2	0.985	0.957 ± 1.11E-02	0.985 ± 3.94E-03	0.954 ± 1.13E-02	0.981 ± 9.41E-03
	3	0.966	0.911 ± 1.22E-02	0.950 ± 8.37E-03	0.900 ± 2.23E-02	0.939 ± 1.51E-02
	4	0.956	0.866 ± 3.28E-02	0.865 ± 4.75E-02	0.878 ± 2.79E-02	0.979 ± 1.86E-02
	5	0.833	0.864 ± 7.10E-03	0.932 ± 7.50E-03	0.796 ± 1.93E-02	0.908 ± 1.27E-02
	6	0.989	0.965 ± 1.23E-02	0.991 ± 5.32E-03	0.936 ± 2.05E-02	0.978 ± 8.23E-03
	7	0.972	0.952 ± 7.73E-03	0.960 ± 6.52E-03	0.945 ± 5.43E-03	0.967 ± 4.95E-03
	8	0.752	0.799 ± 1.14E-02	0.804 ± 7.11E-03	0.664 ± 2.83E-02	0.810 ± 1.22E-02
	9	0.928	0.882 ± 1.83E-02	0.917 ± 1.60E-02	0.910 ± 1.23E-02	0.919 ± 1.28E-02
	10	0.962	0.926 ± 7.11E-03	0.954 ± 6.43E-03	0.934 ± 6.12E-03	0.956 ± 5.48E-03
	11	0.921	0.887 ± 5.67E-03	0.925 ± 6.01E-03	0.880 ± 1.08E-02	0.909 ± 1.26E-02
	12	0.986	0.963 ± 5.18E-03	0.991 ± 1.71E-03	0.973 ± 3.94E-03	0.994 ± 1.89E-03
	13	0.995	0.984 ± 3.31E-03	0.998 ± 6.99E-04	0.972 ± 4.36E-03	0.997 ± 1.35E-03
	14	0.933	0.934 ± 5.57E-03	0.961 ± 4.98E-03	0.862 ± 1.24E-02	0.953 ± 1.24E-02
	15	0.973	0.949 ± 5.82E-03	0.982 ± 3.45E-03	0.937 ± 7.93E-03	0.983 ± 3.47E-03
	16	0.766	0.723 ± 1.32E-02	0.792 ± 1.29E-02	0.719 ± 1.80E-02	0.757 ± 2.42E-02
	17	0.971	0.972 ± 5.54E-03	0.995 ± 1.53E-03	0.935 ± 8.05E-03	0.989 ± 3.72E-03
	18	0.993	0.966 ± 7.05E-03	0.989 ± 2.07E-03	0.976 ± 3.67E-03	0.986 ± 3.59E-03
	19	0.961	0.947 ± 9.30E-03	0.977 ± 7.42E-03	0.929 ± 1.26E-02	0.957 ± 1.17E-02
	20	0.792	0.760 ± 1.94E-02	0.840 ± 1.23E-02	0.709 ± 1.85E-02	0.806 ± 2.02E-02
	21	0.936	0.938 ± 8.41E-03	0.972 ± 2.79E-03	0.919 ± 7.38E-03	0.970 ± 4.90E-03
	22	0.998	0.985 ± 4.18E-03	0.994 ± 1.23E-03	0.983 ± 2.47E-03	0.993 ± 1.35E-03
	23	0.973	0.917 ± 8.22E-03	0.983 ± 3.58E-03	0.901 ± 1.13E-02	0.961 ± 1.01E-02
	24	0.947	0.905 ± 1.22E-02	0.969 ± 4.09E-03	0.893 ± 1.21E-02	0.948 ± 8.20E-03
	25	0.751	0.745 ± 1.90E-02	0.810 ± 1.53E-02	0.701 ± 2.13E-02	0.783 ± 1.79E-02
	26	0.953	0.941 ± 8.28E-03	0.978 ± 3.15E-03	0.883 ± 1.38E-02	0.950 ± 1.65E-02
	27	0.879	0.871 ± 8.20E-03	0.925 ± 1.09E-02	0.777 ± 1.53E-02	0.932 ± 1.04E-02
	28	0.946	0.931 ± 6.92E-03	0.959 ± 4.87E-03	0.873 ± 1.75E-02	0.954 ± 6.73E-03
	29	0.982	0.964 ± 4.26E-03	0.987 ± 2.38E-03	0.956 ± 4.11E-03	0.984 ± 2.60E-03
	30	0.784	0.690 ± 1.83E-02	0.851 ± 1.61E-02	0.669 ± 1.52E-02	0.785 ± 2.76E-02
	31	0.986	0.958 ± 4.97E-03	0.987 ± 3.34E-03	0.920 ± 1.74E-02	0.966 ± 1.06E-02
	32	0.969	0.919 ± 1.20E-02	0.971 ± 4.18E-03	0.929 ± 7.94E-03	0.962 ± 4.78E-03
	33	0.996	0.982 ± 2.61E-03	0.996 ± 1.21E-03	0.982 ± 4.07E-03	0.995 ± 1.24E-03
	34	0.884	0.855 ± 1.04E-02	0.915 ± 8.25E-03	0.806 ± 1.39E-02	0.881 ± 1.34E-02
	35	0.826	0.783 ± 1.21E-02	0.841 ± 1.41E-02	0.748 ± 1.64E-02	0.829 ± 1.78E-02
	36	0.971	0.959 ± 1.16E-02	0.991 ± 2.35E-03	0.954 ± 8.11E-03	0.986 ± 3.46E-03
	37	0.992	0.988 ± 2.96E-03	0.997 ± 6.44E-04	0.979 ± 3.73E-03	0.996 ± 6.81E-04
	38	0.983	0.969 ± 4.66E-03	0.995 ± 1.52E-03	0.945 ± 7.27E-03	0.993 ± 3.42E-03
	39	0.973	0.949 ± 6.47E-03	0.974 ± 4.87E-03	0.934 ± 6.23E-03	0.973 ± 4.17E-03
	40	0.959	0.896 ± 1.28E-02	0.969 ± 5.37E-03	0.896 ± 1.03E-02	0.947 ± 1.18E-02
	41	0.959	0.943 ± 4.86E-03	0.970 ± 3.86E-03	0.901 ± 1.17E-02	0.964 ± 4.88E-03
	42	0.923	0.953 ± 1.17E-02	0.981 ± 5.45E-03	0.884 ± 1.62E-02	0.986 ± 6.30E-03
	43	0.982	0.956 ± 6.68E-03	0.978 ± 4.81E-03	0.966 ± 5.39E-03	0.966 ± 1.07E-02
	44	0.922	0.840 ± 1.75E-02	0.922 ± 1.81E-02	0.794 ± 1.96E-02	0.890 ± 2.62E-02
	45	0.911	0.825 ± 9.49E-03	0.810 ± 3.22E-02	0.853 ± 1.11E-02	0.855 ± 1.46E-02
	46	0.916	0.852 ± 2.08E-02	0.899 ± 1.16E-02	0.870 ± 1.63E-02	0.807 ± 2.54E-02
	47	0.957	0.900 ± 2.66E-02	0.928 ± 1.67E-02	0.899 ± 1.01E-02	0.901 ± 1.72E-02
	48	0.886	0.901 ± 1.14E-02	0.925 ± 9.30E-03	0.854 ± 2.32E-02	0.899 ± 1.34E-02
	49	0.938	0.869 ± 1.40E-02	0.901 ± 9.46E-03	0.918 ± 5.22E-03	0.889 ± 9.64E-03
	50	0.974	0.924 ± 1.53E-02	0.960 ± 6.45E-03	0.955 ± 3.31E-03	0.960 ± 3.73E-03

Finally, we consider the advantage of the data set. In this paper, EEGs were measured from 50 BECTS patients, and 15,899 epileptic spikes and 15,538 non-epileptic discharges were extracted as 1-s segments. To our knowledge, the number of the epileptic spike segments is the largest in the world of epileptic spike detection studies according to the described in Section II-C. This number of the segments strongly supports the credibility of the statistical validation in this paper. For the length of the segment, we set it as 1-s, based on other studies [2], [20] and on the annotation tasks by the five specialists. Of course, there are studies using different length segments [11], [19], however, as the results of this paper show, 1-s extraction is sufficient to achieve a high AUC (> 0.9 in most cases) for BECTS spikes. In particular, since epileptic spike-wave discharges in BECTS patients are known to contain a 3–4 Hz component [32], a segment length of one second can fully contain one of these discharges. Furthermore, even if the position of extracting the spike waveform is slightly misaligned, it is unlikely that any part of the waveform will be lost, thus the 1-s extraction is appropriate.

In conclusion, we proposed a method to combine a bank of linear-phase filters with a convolutional neural network and learn its coefficients from the data. To our knowledge, we have built the largest dataset in the literature, containing 31,437

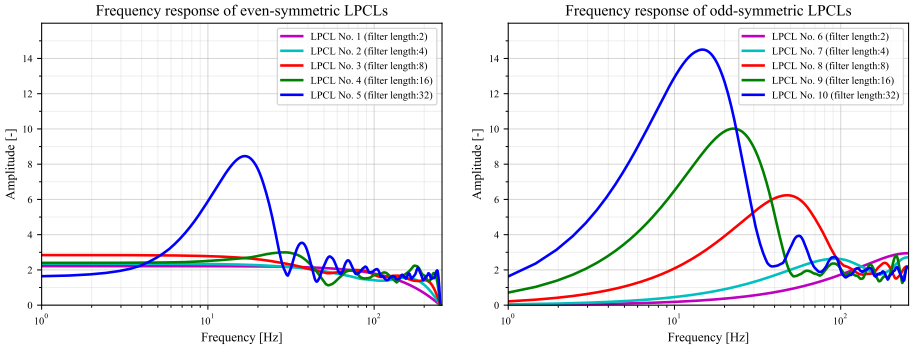

(a) Even-symmetric LPCLs (LPCL No. 1 to 5) (b) Odd symmetric LPCLs (LPCL No. 6 to 10)

Fig. 6. An example of mean filter spectrums at the LPCL combining with ANN.

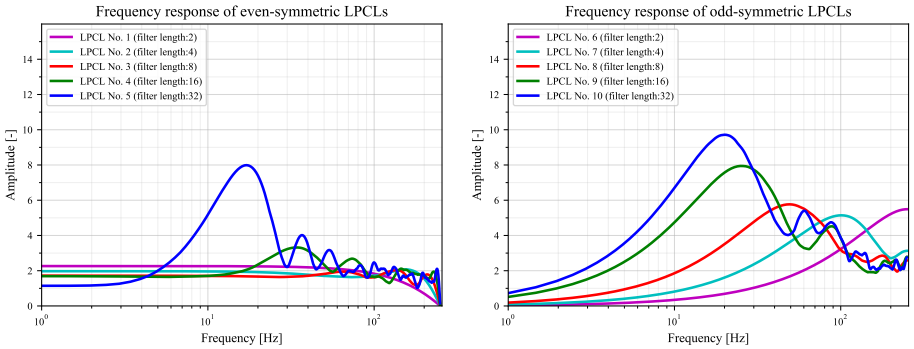

(a) Even-symmetric LPCLs (LPCL No. 1 to 5) (b) Odd-symmetric LPCLs (LPCL No. 6 to 10)

Fig. 7. An example of mean filter spectrums at the LPCL combining with CNN.

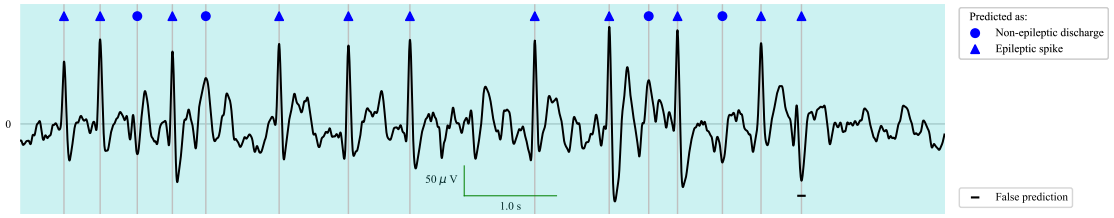

Fig. 8. An example of predicted spikes. The circles and triangles indicate non-epileptic discharges and epileptic spikes, respectively. A bar at the bottom indicates that the classification failed.

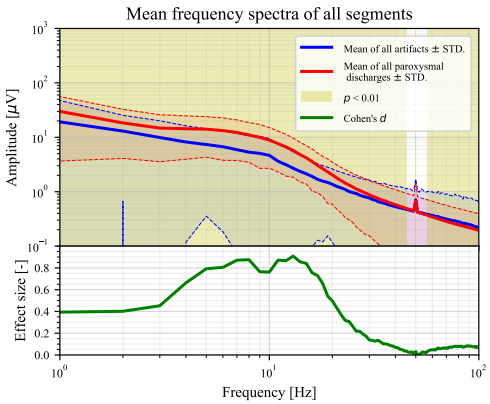

Fig. 9. The mean spectrum of all 15,538 segments of non-epileptic discharges and the mean spectrum of all 15,899 segments of epileptic spikes. The areas where $p < 0.01$ in the t-test between the two classes at each frequency are filled in yellow, and the bottom of the graph shows its effect size.

samples annotated by two neurosurgeons, two clinical technologists, and one pediatrician. The proposed model classify 1-s segments to epileptic spikes or non-epileptic discharges with high performance (AUC $>$ 0.9 in most cases). Furthermore, the frequency response of the filter fitted from the EEG is strongly responds in the low frequency range (around 14 Hz). This band coincided brilliantly with the frequency band of interest in the raw EEG segments of epileptic spikes.

REFERENCES

[1] F. A. El-Samie, T. N. Alotaiby, M. Khalid, S. A. Alshebeili, and S. Aldosari, "A review of EEG and MEG epileptic spike detection algorithms," *IEEE Access*, vol. 6, pp. 60673–60688, 2018.

[2] J. E. Le Douget, A. Fouad, M. M. Filali, J. Pyrzowski, and M. Le Van Quyen, "Surface and intracranial EEG spike detection based on discrete wavelet decomposition and random forest classification," *2017 39th Annual International Conference of the IEEE Engineering in Medicine and Biology Society (EMBC)*, pp. 475–478, 2017.

[3] H. J. Carey, M. Manic, and P. Arsenovic, "Epileptic spike detection with EEG using artificial neural networks," in *2016 9th International Conference on Human System Interactions (HSI)*, July 2016, pp. 89–95.

[4] I. Ullah, M. Hussain, E. Qazi, and H. Aboalsamh, "An automated system for epilepsy detection using EEG brain signals based on deep learning approach," *Expert Systems with Applications*, vol. 107, pp. 61–71, 2018.
[5] K. Fukumori, H. T. Thu Nguyen, N. Yoshida, and T. Tanaka, "Fully data-driven convolutional filters with deep learning models for epileptic spike detection," in *2019 IEEE International Conference on Acoustics, Speech and Signal Processing (ICASSP)*, May 2019, pp. 2772–2776.
[6] J. Gutiérrez, R. Alcántara, and V. Medina, "Analysis and localization of epileptic events using wavelet packets," *Medical Engineering and Physics*, vol. 23, pp. 623–631, 2001.
[7] V. Nigam and D. Graupe, "A neural-network-based detection of epilepsy," *Neurological Research*, vol. 26 1, pp. 55–60, 2004.
[8] I. Omerhodzic, S. Avdakovic, A. Nuhanovic, K. Dizdarevic, and K. Rotim, "Energy distribution of EEG signal components by wavelet transform," in *Wavelet Transforms and Their Recent Applications in Biology and Geoscience*, Dumitru Baleanu, Ed., chapter 2. IntechOpen, Rijeka, 2012.
[9] Y. U. Khan, N. Rafiuddin, and O. Farooq, "Automated seizure detection in scalp EEG using multiple wavelet scales," in *2012 IEEE International Conference on Signal Processing, Computing and Control*, March 2012, pp. 1–5.
[10] E. Juárez-Guerra, V. Alarcon-Aquino, and P. Gómez-Gil, "Epilepsy seizure detection in EEG signals using wavelet transforms and neural networks," in *New Trends in Networking, Computing, E-learning, Systems Sciences, and Engineering*, Khaled Elleithy and Tarek Sobh, Eds., Cham, 2015, pp. 261–269, Springer International Publishing.
[11] L. Xuyen, L. Thanh, D. Viet, T. Long, N. Trung., and N. Thuan, "Deep learning for epileptic spike detection," *VNU Journal of Science: Computer Science and Communication Engineering*, vol. 33, no. 2, 2018.
[12] L. T. Thanh, N. T. Anh Dao, N. V. Dung, N. L. Trung, and K. Abed-Meraim, "Multi-channel EEG epileptic spike detection by a new method of tensor decomposition," *Journal of Neural Engineering*, vol. 17, no. 1, pp. 016023, Jan. 2020.
[13] C. Cheong, R. Sudirman, and S. S. Hussin, "Feature extraction of EEG signals using wavelet transform for autism classification," *Journal of Engineering and Applied Sciences*, vol. 10, no. 9, 2015.
[14] K. Polat and S. Günes, "Classification of epileptiform EEG using a hybrid system based on decision tree classifier and fast fourier transform," *Applied Mathematics and Computation*, vol. 187, pp. 1017–1026, 2007.
[15] K. P. Indiradevi, Elizabeth Elias, P. S. Sathidevi, S. Dinesh Nayak, and K. Radhakrishnan, "A multi-level wavelet approach for automatic detection of epileptic spikes in the electroencephalogram," *Computers in Biology and Medicine*, vol. 38 7, pp. 805–816, 2008.
[16] P. Fergus, D. Hignett, A. J. Hussain, D. Al-Jumeily, and K. Abdel-Aziz, "Automatic epileptic seizure detection using scalp EEG and advanced artificial intelligence techniques," in *BioMed Research International*, 2015.
[17] K. Simonyan and A. Zisserman, "Two-stream convolutional networks for action recognition in videos," in *Proceedings of the 27th International Conference on Neural Information Processing Systems*, Cambridge, MA, USA, 2014, vol. 1 of *NIPS'14*, pp. 568–576, MIT Press.
[18] A. Qayyum, S. M. Anwar, M. Awais, and M. Majid, "Medical image retrieval using deep convolutional neural network," *Neurocomputing*, vol. 266, pp. 8–20, 2017.
[19] A. R. Johansen, J. Jin, T. Maszczyk, J. Dauwels, S. S. Cash, and M. B. Westover, "Epileptiform spike detection via convolutional neural networks," in *2016 IEEE International Conference on Acoustics, Speech and Signal Processing (ICASSP)*, March 2016, pp. 754–758.
[20] M. Zhou, C. Tian, C. Rui, B. Wang, Y. Niu, T. Hu, H. Guo, and J. Xiang, "Epileptic seizure detection based on EEG signals and CNN," *Frontiers in Neuroinformatics*, vol. 12, 12 2018.
[21] S. B. Wilson, C. A. Turner, R. G. Emerson, and M. L. Scheuer, "Spike detection II: automatic, perception-based detection and clustering," *Clinical neurophysiology : official journal of the International Federation of Clinical neurophysiology*, vol. 110, no. 3, pp. 404–411, March 1999.
[22] Y. C. Liu, C. C. K. Lin, J. J. Tsai, and Y. N. Sun, "Model-based spike detection of epileptic EEG data," *Sensors*, vol. 13, no. 9, pp. 12536–12547, September 2013.
[23] W. D. Shields and O. C. Snead III, "Benign epilepsy with centrotemporal spikes," *Epilepsia*, vol. 50, no. s8, pp. 10–15, August 2009.
[24] L. H. Negri and C. Vestri, "lucashn/peakutils: v1.1.0," September 2017.
[25] J. E. Jacob, G. K. Nair, T. Iype, and A. Cherian, "Diagnosis of encephalopathy based on energies of EEG subbands using discrete wavelet transform and support vector machine," *Neurology Research International*, 2018.
[26] M. Mahadevappa D. Sikdar, R. Roy, "Epilepsy and seizure characterisation by multifractal analysis of EEG subbands," *Biomedical Signal Processing and Control*, vol. 41, pp. 264–270, 2018.
[27] K. He, X. Zhang, S. Ren, and J. Sun, "Delving deep into rectifiers: Surpassing human-level performance on imagenet classification," in *Proceedings of the 2015 IEEE International Conference on Computer Vision (ICCV)*, Washington, DC, USA, 2015, ICCV '15, pp. 1026–1034, IEEE Computer Society.
[28] X. Glorot and Y. Bengio, "Understanding the difficulty of training deep feedforward neural networks," in *Proceedings of the Thirteenth International Conference on Artificial Intelligence and Statistics*, 2010, pp. 249–256.
[29] S. Siegel and N.J. Castellan, *Nonparametric statistics for the behavioral sciences*, McGraw–Hill, Inc., second edition, 1988.
[30] G. D. Ruxton, "The unequal variance t-test is an underused alternative to Student's t-test and the Mann–Whitney U test," *Behavioral Ecology*, vol. 17, no. 4, pp. 688–690, 05 2006.
[31] J Cohen, *Statistical Power Analysis for the Behavioral Sciences*, Routledge, second edition, 1988.
[32] J. S. Hahn, "Neonatal and pediatric electroencephalography," in *Aminoff's Electrodiagnosis in Clinical Neurology (Sixth Edition)*, M. J. Aminoff, Ed., pp. 85–128. W.B. Saunders, London, sixth edition edition, 2012.